

JAERI - M
82-004

COMPARISON OF CALCULATIONS FOR THE
ROSA-IV LSTF WITH RELAP5 / MOD 0 AND
RELAP5 / MOD 1 (CYCLE 1)

— 10% AND 2.5% COLD LEG BLEAK —

March 1982

C.P.FINEMAN*, Mitsugu TANAKA and Kanji TAsAKA

日本原子力研究所
Japan Atomic Energy Research Institute

JAERI-Mレポートは、日本原子力研究所が不定期に公刊している研究報告書です。
入手の問い合わせは、日本原子力研究所技術情報部情報資料課（〒319-11茨城県那珂郡東海村）あて、お申しこしください。なお、このほかに財団法人原子力弘済会資料センター（〒319-11茨城県那珂郡東海村日本原子力研究所内）で複写による実費頒行をおこなっております。

JAERI-M reports are issued irregularly.

Inquiries about availability of the reports should be addressed to Information Section, Division of Technical Information, Japan Atomic Energy Research Institute, Tokai-mura, Naka-gun, Ibaraki-ken 319-11, Japan.

©Japan Atomic Energy Research Institute, 1982

編集兼発行 日本原子力研究所
印刷 株式会社 高野高速印刷

JAERI-M 82-004

Comparison of Calculations for the ROSA-IV
LSTF with RELAP5/MOD0 and RELAP5/MOD1 (cycle 1)
—— 10% and 2.5% Cold Leg Break ——

C.P. FINEMAN^{*}, Mitsugu TANAKA and Kanji TASAKA

Division of Reactor Safety,
Tokai Research Establishment, JAERI

(Received January 29 , 1982)

10% and 2.5% cold leg break analyses have been completed for the ROSA-IV Large Scale Test Facility (LSTF) with the RELAP5/MOD0 and RELAP5/MOD1, cycle 1, computer codes. Comparisons between the calculations were made to determine any differences in the results obtained from the two versions of RELAP5. Differences in the two calculations were found which can be attributed to changes in the flow regime maps and critical flow model.

Keywords: ROSA-IV, LSTF, LOCA, Small-Break, RELAP5, Computer Analysis, Comparative Evaluations

* USNRC sponsored delegate to the ROSA-IV Program

ROSA-W LSTFに対するRELAP 5/MOD 0とRELAP 5/MOD 1 (cycle 1)
による予備計算の比較検討

—— 10%と2.5%コールドレグ破断 ——

日本原子力研究所東海研究所安全工学部
C. P. FINEMAN^{*}・田中 貢・田坂完二

(1982年1月29日受理)

RELAP 5/MOD 0とRELAP 5/MOD 1 (cycle 1)コードにより、ROSA-W LSTF (Large Scale Test Facility) の10%および2.5%コールドレグ破断を解析し、その結果を比較検討した。MOD 0コードとMOD 1コードの計算結果の差異は大きくないが、その差異は主として2相流流動様式の判別条件および臨界流モデルの差異によると考えられた。

*日米軽水炉安全性情報交換協定に基づく派遣研究員 (EG & G Idaho, Inc.)

CONTENTS

1. INTRODUCTION	1
2. OBJECTIVES AND DESIGN PHILOSOPHY OF ROSA-IV LSTF	3
2.1 Objectives	3
2.2 Design Philosophy	4
3. RELAP5 MODEL DESCRIPTION OF THE LSTF	11
3.1 RELAP5/MOD0 Model	11
3.2 RELAP5/MOD1 Model	12
3.3 Trip Logic	14
4. ANALYSIS OF CALCULATED RESULTS	18
4.1 10% Cold Leg Break Calculations	19
4.2 2.5% Cold Leg Break Calculations	22
5. CONCLUSIONS	35
ACKNOWLEDGEMENTS	35
REFERENCES	36

目 次

1. 序	1
2. ROSA-N LSTFの目的と設計方針	3
2.1 目的	3
2.2 設計方針	4
3. LSTFのRELAP 5 モデル	1 1
3.1 RELAP 5 /MOD 0モデル	1 1
3.2 RELAP 5 /MOD 1モデル	1 2
3.3 トリップ条件	1 4
4. 計算結果の検討	1 8
4.1 10%コールドレグ破断の計算	1 9
4.2 2.5%コールドレグ破断の計算	2 2
5. 結論	3 5
謝辞	3 5
参考文献	3 6

List of Tables

- Table 2.1 Major Characteristics of Large Scale Test Facility (LSTF) as of November 1981.
- Table 2.2 Elevation of Each Position
- Table 4.1 Table of Significant Events (10% Break)
- Table 4.2 Table of Significant Events (2.5% Break)

List of Figures

- Fig.2.1 Experimental Instrumentation Flow Diagram
- Fig.3.1 Nodalization of LSTF (MOD0 Calculation)
- Fig.3.2 Nodalization of LSTF (MOD1 Calculation)
- Fig.4.1 Comparison of S.G. Secondary Pressure between MOD0 and MOD1.
- Fig.4.2 Comparison of S.G. Secondary Outlet Flow between MOD0 and MOD1.
- Fig.4.3 Comparison of Upper Plenum Pressure between MOD0 and MOD1.
- Fig.4.4 Comparison of S.G. Secondary Heat Transfer between MOD0 and MOD1.
- Fig.4.5 Comparison of Break Flow between MOD0 and MOD1.
- Fig.4.6 Comparison of Density Upstream of the Break between MOD0 and MOD1.
- Fig.4.7 Comparison of Rod Surface Temperature between MOD0 and MOD1.
- Fig.4.8 Comparison of Void Fraction in the Core between MOD0 and MOD1.
- Fig.4.9 Comparison of Core Inlet Flowrate between MOD0 and MOD1.

- Fig.4.10 Comparison of Total Mass in Primary Loop between MOD0 and MOD1.
- Fig.4.11 Comparison of S.G. Secondary Pressure between MOD0 and MOD1.
- Fig.4.12 Comparison of S.G. Secondary Outlet Flow between MOD0 and MOD1.
- Fig.4.13 Comparison of Upper Plenum Pressure between MOD0 and MOD1.
- Fig.4.14 Comparison of Vapor Mass in Primary Loop between MOD0 and MOD1.
- Fig.4.15 Comparison of Density Upstream of the Break between MOD0 and MOD1.
- Fig.4.16 Comparison of Break Flowrate between MOD0 and MOD1.
- Fig.4.17 Comparison of Rod Surface Temperature between MOD0 and MOD1.
- Fig.4.18 Comparison of Void Fraction in the Core between MOD0 and MOD1.
- Fig.4.19 Comparison of Core Inlet Flowrate between MOD0 and MOD1.
- Fig.4.20 Comparison of Total Mass in Primary Loop between MOD0 and MOD1.

1. INTRODUCTION

Since the accident at Three Mile Island - Unit 2 (TMI-2) the interest of the reactor safety research community has been reorientated from the large break loss-of-coolant accident (LOCA) to the small break LOCA and anticipated transient. In keeping with this interest, the Japan Atomic Energy Research Institute (JAERI) has instituted the Rig of Safety Assessment, Number 4 (ROSA-IV) Program to study the thermal-hydraulic phenomena and plant parameters which affect the performance of a pressurized water reactor (PWR) during a small break LOCA. The ROSA-IV program includes the Two-Phase Test Facility (TPTF) which is a separate effects test facility and the Large Scale Test Facility^[1] (LSTF) which will be used to conduct integral and system effects tests.

As part of the design process for the LSTF, calculations for a 10% and 2.5% cold leg break were completed with the RELAP5/MOD0^[2] computer code. These calculations were reported in references [3] and [4]. Since those calculations were completed, RELAP5/MOD1, cycle 1,^[5] has become available at JAERI and the calculations were repeated using this later version of the code. Since the information from the MOD0 calculations was factored into the design of the LSTF, it was very important to know if there were any differences in the results calculated with MOD0 and MOD1. This report describes the results of comparing the MOD0 calculated results and the MOD1 calculated results.

Section 2 of this report contains a brief description of the ROSA-IV program and its objectives. The models used in

making the computer calculations are described briefly in Section 3 and Section 4 contains the results of the analysis. The main conclusions are presented in Section 5.

2. OBJECTIVES AND DESIGN PHILOSOPHY OF ROSA-IV LSTF

2.1 Objectives

The purpose of tests to be performed at LSTF is to provide test data from a large-scale test facility on the transient performance of PWRs under small break loss-of-coolant accident (SBLOCA) and transient conditions and on the effectiveness of emergency safeguard systems and procedures under such conditions. The tests will also provide experimental data on two-phase fluid flow in PWRs. Specifically, LSTF will be used to:

- (1) Study the effectiveness of the ECCS under SBLOCA and plant transient conditions. Both standard and potential alternate ECCS will be evaluated.
- (2) Study the effectiveness of secondary side cooling via the steam generators under SBLOCA and plant transient conditions.
- (3) Examine the nature of forced and natural circulation cooling in PWRs in various flow regimes and cooling modes and in transition from one flow regime or mode of cooling to another.
- (4) Examine the effect of break size and location on system behavior.
- (5) Study the effects of non-condensable gases on system behavior during a SBLOCA or plant transient.
- (6) Investigate alternate design systems and/or procedures which are being considered to improve system performance during SBLOCA and/or plant transient.
- (7) Provide test data with which to develop/verify the SBLOCA

analytical model being developed in connection with the ROSA-IV Program.

2.2 Design Philosophy

LSTF is an experimental test facility designed to model a full height primary system of an LPWR. The reference PWR for LSTF is a 1100 MWe (3423 MWt) PWR with 50,952 fuel pins arranged in 17×17 square lattices. The scale factor for LSTF is 1/48. Scaling of LSTF is accomplished as follows:

- a. Elevations are preserved, i.e., the scaling ratio is 1/1. Preserving correct elevations is important to LSTF, since gravity strongly influences PWR long-term transient behavior, for instance, natural circulation.
- b. Volumes are scaled by the facility scale factor of 1/48.
- c. Flow Area in the pressure vessel and steam generators are scaled by the facility scale factor of 1/48 and 1/24, respectively. But the flow area of the primary loop, i.e., hot-leg and cold-leg, was determined from the conservation of the volume scaling and the Strouhal number so that the flow regime transition can be simulated.
- d. Core Power is scaled by the facility scale factor of 1/48 so that the power input per unit volume in the core region is the same as for the reference PWR. Note, for full power operation, the scaled power of the core would be 71 MW. However, heater rod power supply is limited to 10 MW. Hence, proper core power scaling can only be attained for simulator core power starting at about 14%

full power.

- e. Fuel Assembly dimensions, i.e., fuel rod diameter, pitch and length, guide thimble diameter pitch and length, and ratio of number of fuel rods to number of guide thimbles, are the same as for the 17×17 fuel assembly of the reference PWR in order to preserve the heat transfer characteristics of the core. The total number of rods is scaled by the facility scale factor and is 1080 heated and 104 unheated rods.
- f. Design Pressures for the LSTF fluid systems will be at least the same as those for their counterparts in the reference PWR.
- g. Fluid Flow Δ Ps of major components, e.g., pumps, pressure vessel and steam generators will be the same as in the reference PWR.
- h. Flow Capacities for LSTF systems are scaled by the power scale factor to the enthalpy distribution.

Major characteristics of LSTF are shown in Tables 2.1, 2.2 and the flow diagram is shown in Fig.2.1.

Table 2.1 Major Characteristics of Large Scale Test Facility
(LSTF) as of November 1981.

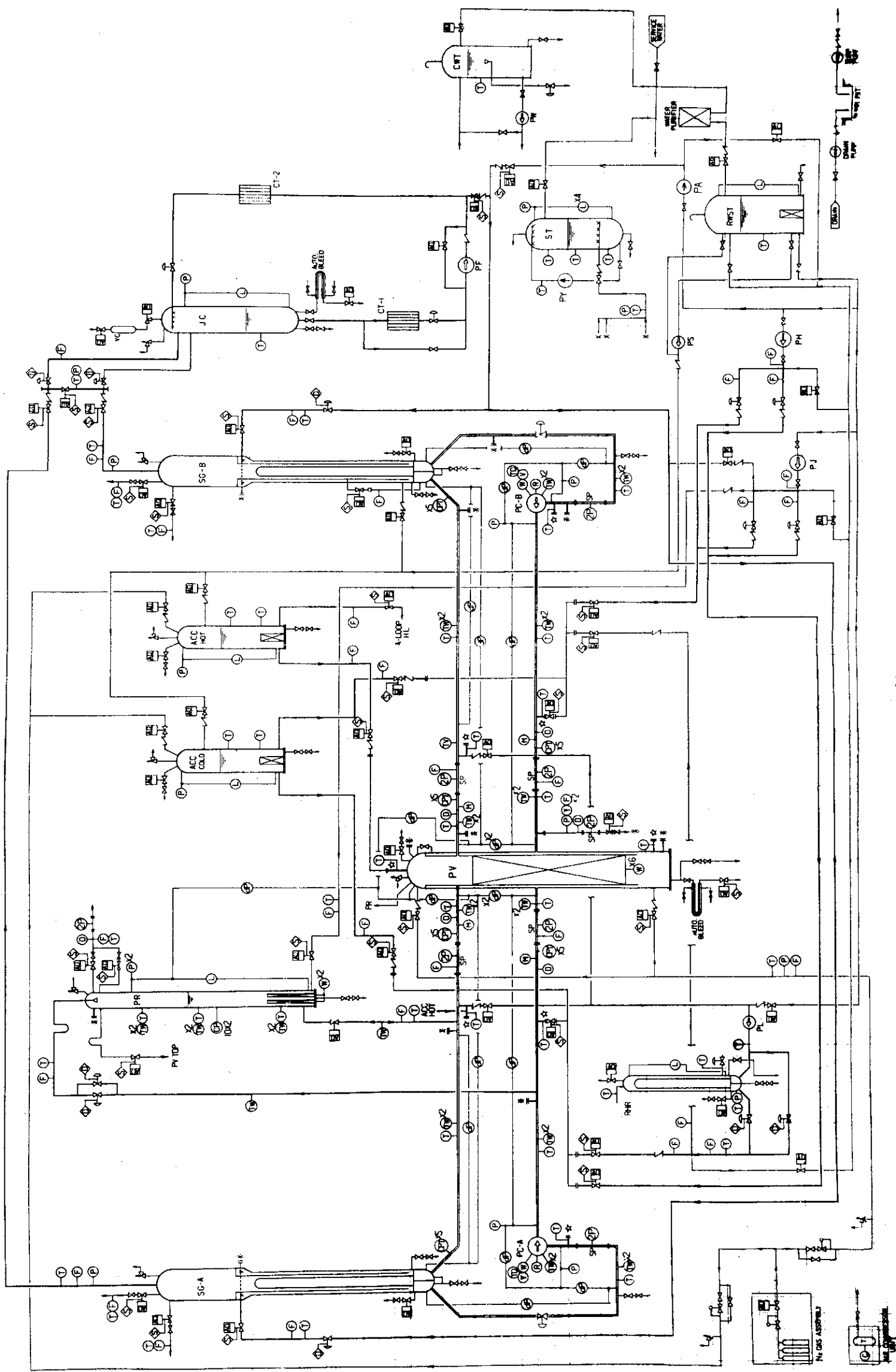
COMPONENT	PWR	LSTF	SCALE
PRESSURE VESSEL			
VESSEL INSIDE DIAMETER (mm)	4394	640	1/6.87
VESSEL THICKNESS (mm)	216		
CORE BARREL OUTSIDE DIAMETER (mm)	3874	520	1/7.45
DOWNCOMER LENGTH (mm)	6066	6066	1/1
DOWNCOMER GAP (mm)	260	60	1/4.33
DOWNCOMER FLOW AREA (m ²)	3.38	0.109	1/31.0
LOWERPLENUM FLUID VOLUME (PV INSIDE VOLUME) (m ³)	29.6	0.62	1/48
UPPER PLENUM FLUID VOLUME (NOT INCLUDE UPPER HEAD VOLUME) (m ³)	28.4	0.60	1/48
UPPER HEAD FLUID VOLUME (m ³)	24.6	0.51	1/48
FUEL (HEATER ROD) ASSEMBLY			
NUMBER OF BUNDLES	193	24	
ROD ARRAY	17 x 17	7 x 7	
ROD HEATED LENGTH (mm)	3660	3660	1/1
ROD PITCH (mm)	12.6	12.6	1/1
FUEL ROD OUTSIDE DIAMETER (mm)	9.5	9.5	1/1
THIMBLE TUBE DIAMETER (mm)	12.24	12.2	1/1
INSTRUMENT TUBE DIAMETER (mm)	12.24	12.2	1/1
NUMBER OF HEATER RODS	50952	1080	1/47.2
NUMBER OF NON-HEATING RODS	4825	104	1/46.4
CORE FLOW AREA (WITHOUT SPACER LOCATION) (m ²)	4.75	0.107	1/44.4
CORE FLOW AREA (WITH SPACER LOCATION) (m ²)	3.70		
CORE FLUID VOLUME (m ³)	17.5	0.392	1/44.6
PRIMARY LOOP (SAME 2 LOOPS)			
HOT LEG INSIDE DIAMETER (mm)	736.6	207	
HOT LEG LENGTH (mm)	7040	3730	L/√D SIMULATED
CROSSOVER LEG			
INSIDE DIAMETER (mm)	787.4	207	
LENGTH (mm)	10280	5270	
COLD LEG INSIDE DIAMETER (mm)	698.5	207	
COLD LEG LENGTH (mm)	8400	4570	

Table 2.1 (CONTINUED)

COMPONENT		PWR	LSTF	SCALE
PRESSURIZER				
VESSEL INSIDE DIAMETER	(mm)	2100	600	1/3.5
VESSEL HEIGHT	(mm)	15500	4200	1/3.69
TOTAL VOLUME	(m ³)	51	1.1	1/48
FLUID VOLUME	(m ³)	31	0.65	1/48
ACCUMULATOR (COLD AND HOT)				
VESSEL INSIDE DIAMETER	(mm)	3500	950	1/3.68
VESSEL HEIGHT	(mm)	5280	6600	1.25
TOTAL VOLUME	(m ³)	38.2	4.8	1/7.96
LIQUID VOLUME	(m ³)	26.9	3.38	1/7.96
RHR HEAT EXCHANGER				
NUMBER OF TUBES/1PASS		568	24	1/23.7
TOTAL U TUBE LENGTH	(mm)	8600	8600	1/1
TUBE OUTSIDE DIAMETER	(mm)	19.0		
TUBE INSIDE DIAMETER	(mm)	16.6		
TUBE WALL THICKNESS	(mm)	1.2		
TUBE PITCH	(mm)	28.5	28.5	1/1
TUBE ARRAY		Δ	Δ	
HEAT TRANSFER AREA (OUTER SURFACE)	(m ²)	590	25	1/23.6
STEAM GENERATOR (SAME 2 S.G s)				
NUMBER OF TUBES		3382	141	1/24
TUBE LENGTH (AVERAGE)	(m)	20.24	20.24	1/1
TUBE OUTSIDE DIAMETER	(mm)	22.23	25.4	
TUBE INSIDE DIAMETER	(mm)	19.7	19.6	1/1
TUBE WALL THICKNESS	(mm)	1.27	2.9	
HEAT TRANSFER AREA (OUTER SURFACE OF TUBE)	(m ²)	4784	199	1/24
INLET PLENUM VOLUME	(m ³)	4.25	0.18	1/24
OUTLET PLENUM VOLUME	(m ³)	4.25	0.18	1/24
PRIMARY SIDE VOLUME	(m ³)	29.36	1.22	1/24
SECONDARY SIDE VOLUME	(m ³)	157.33	6.56	1/24

Table 2.2 Elevation of Each Position

POSITION		PWR	LSTF	SCALE
BOTTOM OF HEATER BUNDLE	(mm)	0	0	
TOP OF HEATER BUNDLE	(mm)	3660	3660	1/1
TOP OF DOWNCOMER	(mm)	4849	4849	1/1
BOTTOM OF DOWNCOMER	(mm)	-1217	-1217	1/1
CENTER OF COLD LEG	(mm)	5198		
TOP OF COLD LEG INSIDE DIAMETER (CROSS OVER LEG)	(mm)	5548	5548	1/1
CENTER OF LOOP SEAL LOWER END	(mm)	2056		
BOTTOM OF LOOP SEAL LOWER END	(mm)	1662	1662	1/1
CENTER OF HOT LEG	(mm)	5198		
TOP OF HOT LEG INSIDE DIAMETER	(mm)	5567	5567	1/1
BOTTOM OF UPPER CORE PLATE	(mm)	3957	3957	1/1
TOP OF LOWER CORE PLATE	(mm)	-108	-108	1/1
BOTTOM OF TUBE SHEET OF STEAM GENERATOR	(mm)	7308	7308	1/1
PLENUM LOWER END OF STEAM GENERATOR	(mm)	5713	5713	1/1
TOP OF TUBES OF STEAM GENERATOR (AVG)	(mm)	17953	17953	1/1



B-LOOP

A-LOOP

Fig.2.1 Experimental Instrumentation Flow Diagram

3. RELAP5 MODEL DESCRIPTION OF THE LSTF

This section describes briefly the RELAP5 models used to make the calculations for this study. The model for the RELAP5/MOD0 calculations is described first. The model for the RELAP5/MOD1 calculations was made from the MOD0 model and therefore only the changes to the MOD0 model will be discussed. Finally the trip logic used in the calculations will be described.

3.1 RELAP5/MOD0 Model

A nodalization diagram of the RELAP5/MOD0 model of the LSTF is shown in Figure 3.1. The model included 114 volumes and 117 junctions. Structural heat transfer in the vessel and heat transfer in the core and steam generators were represented by 26 heat structures.

Initial thermal-hydraulic conditions for the calculations were obtained from calculated results and engineering analysis of the steady-state problem. To be properly scaled the core power for LSTF would have to be 71.3 MW. However, local utility limitations will only allow an initial core power of 10 MW. This affected the steady-state calculation in several ways. First, in order to maintain the LSTF steam generator secondary pressure the same as the reference plant out only remove 10 MW at steady-state, the mixture level in the secondary was lowered to 58 cm. Second, the pumps were turned off and natural circulation was used to obtain the flowrate which would give the proper temperature distribution in the loop. However, since the

natural circulation flowrate was still larger than the desired flowrate, valves were added to the cold legs with an area of 0.00023 m^2 to get the proper flowrate. This compares with the nominal cold leg area of 0.0302 m^2 . These valves were only used during the steady state calculation. The temperatures of the cold and hot legs were set to give the same core temperature rise as the reference PWR and were consistent with the flowrate and 10 MW core power. The core temperature distribution was determined based on the enthalpy rise through the core and considered the distribution of the energy transferred from the rods.

A parameter survey was completed to determine the energy loss coefficients needed in the steam generator steam line to remove 10 MW energy (5 MW/steam generator) at steady-state. To perform the transient calculation, the steam line model was changed to represent 71.3 MW energy removal to simulate the PWR. This was done by adjusting the junction and volume flow areas and leaving the energy loss coefficients the same.

3.2 RELAP5/MOD1 Model

Since the purpose of repeating the RELAP5/MOD0 calculations with MOD1, cycle 1, was to compare the results, it was desirable to make as few changes as possible to the model and still be able to run with the MOD1 version of the program. Therefore the following changes to the MOD0 model were made:

1. Input changes required to run with MOD1 including: an additional word for pipe initial conditions

- (boron concentration), the valve input was made consistent with the MOD1 card sequence, and composition and source distribution flags from heat structure input were deleted.
2. Additional trip and time dependent junction capabilities (e.g., trip controlled time dependent junction flow) were used so that the calculation could be completed with a single run using RELAP5/MOD1.
 3. An error message from the heat structure initialization indicating inconsistent right and left surface areas for certain heat structures was corrected by inputting length instead of surface area. On initialization the surface areas calculated by RELAP5 were compared to the MOD0 input and were essentially the same.
 4. Trips which referenced steam generator secondary pressure were corrected so they referenced the steam dome pressure instead of the bottom of the secondary.
 5. The accumulator model available in RELAP5/MOD1, cycle 1, was input into the model instead of the time dependent volume used in the MOD0 model. This change does not affect the calculated results, however, because both the MOD0 and the MOD1 calculations were terminated at the beginning of accumulator injection.

The initial thermal-hydraulic conditions for the RELAP5/MOD1 calculations were obtained from a steady-state calculation completed with MOD1. This calculation used the control system available with the MOD1 version of RELAP5 to control a servo valve at the steam generator exit to obtain the steam flow rate needed to give the correct cold leg temperature. To get a steady

state with RELAP5/MOD1 two additional input changes to the MOD0 data were needed. First, in order to get the correct steam generator secondary pressure, the mass in the secondary had to be increased by approximately 100 kg resulting in a collapsed secondary level of 94 cm. Second, in order to get the correct primary system flowrate, the area of the valves in the cold legs had to be reduced slightly (0.00023 to 0.00021 m²). This gave the correct core temperature difference, but the resulting core temperature distribution was different from the MOD0 transient calculation input. This was because RELAP5 uses average volume properties and therefore all the energy transferred from the rods in a volume to the fluid is reflected in the volume fluid temperature. Therefore while the same core temperature difference was maintained in the MOD1 calculation, the fluid temperature of each of the individual core volumes was higher than the fluid temperature in the corresponding volume in the MOD0 calculation.

To maintain similarity in the transient models, the same energy loss coefficients and junction and volume flow areas were used in the MOD1 calculations as were used in the MOD0 calculations.

3.3 Trip Logic

The trip logic used to control the steam generators and the plant protection systems (core trip and emergency core cooling systems (ECCS)) were based on the trip logic for the reference plant. These are described below:

	<u>Action</u>	<u>Setpoint</u>
①	PWR scram	$P < 12.97 \text{ MPa}$ ^a
②	Trip coolant pump and main FW, initiate safety injection and aux FW trips	$P < 12.27 \text{ MPa}$ ^a
③	LSTF core power trip	① + 7.1 s
④	Safety injection begins	② + 17.0 s
⑤	Aux FW begins	② + 28.0 s
⑥	Main steam isolation valve closes	$P < 4.325 \text{ MPa}$ ^b
⑦	Accumulator injection begins	$P < 4.51 \text{ MPa}$ ^c

a. Pressurizer pressure

b. Steam generator secondary steam dome pressure

c. Pressure in cold leg downstream of accumulator

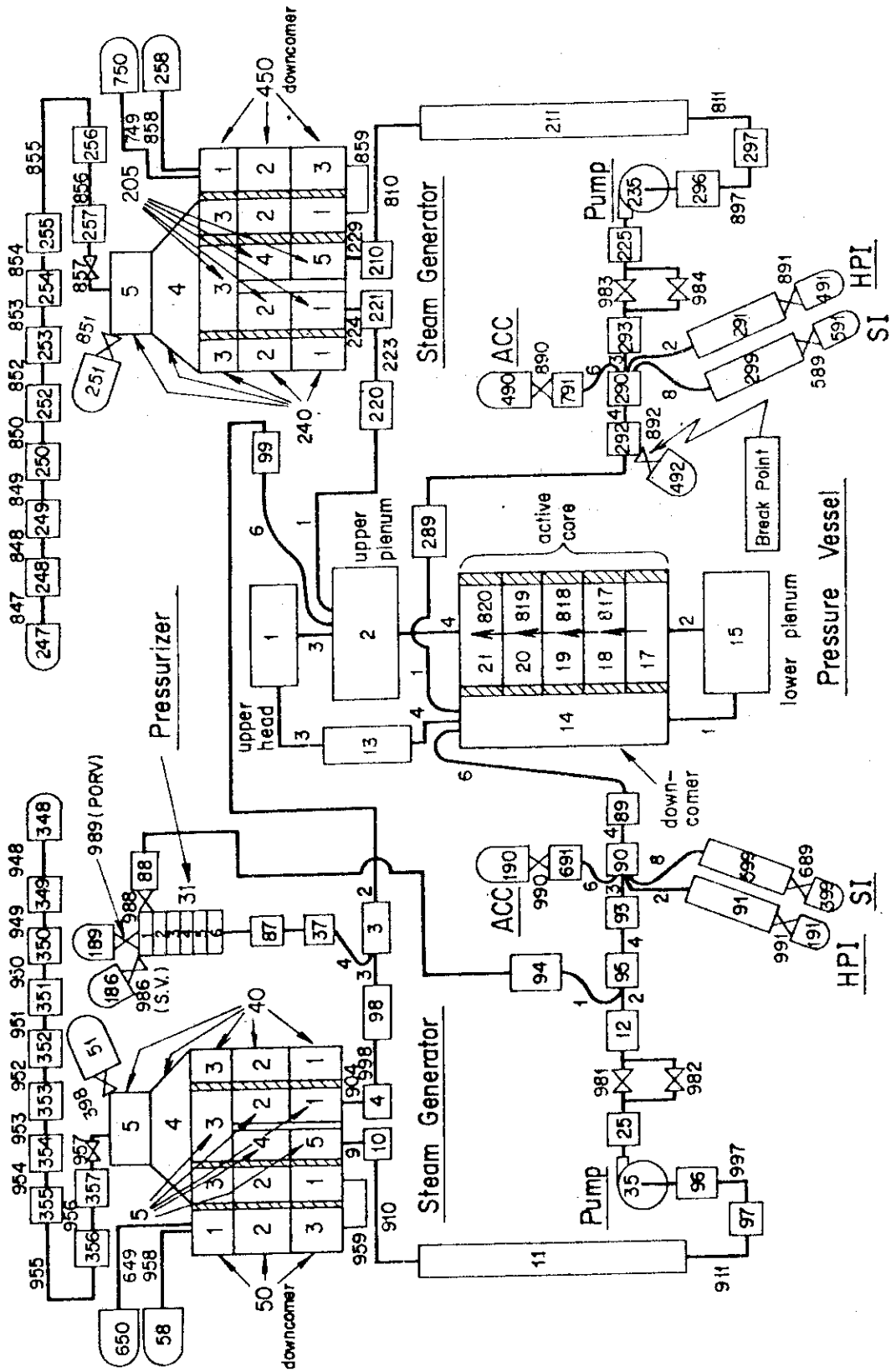


Fig.3.1 Nodalization of LSTF (MOD0 Calculation)

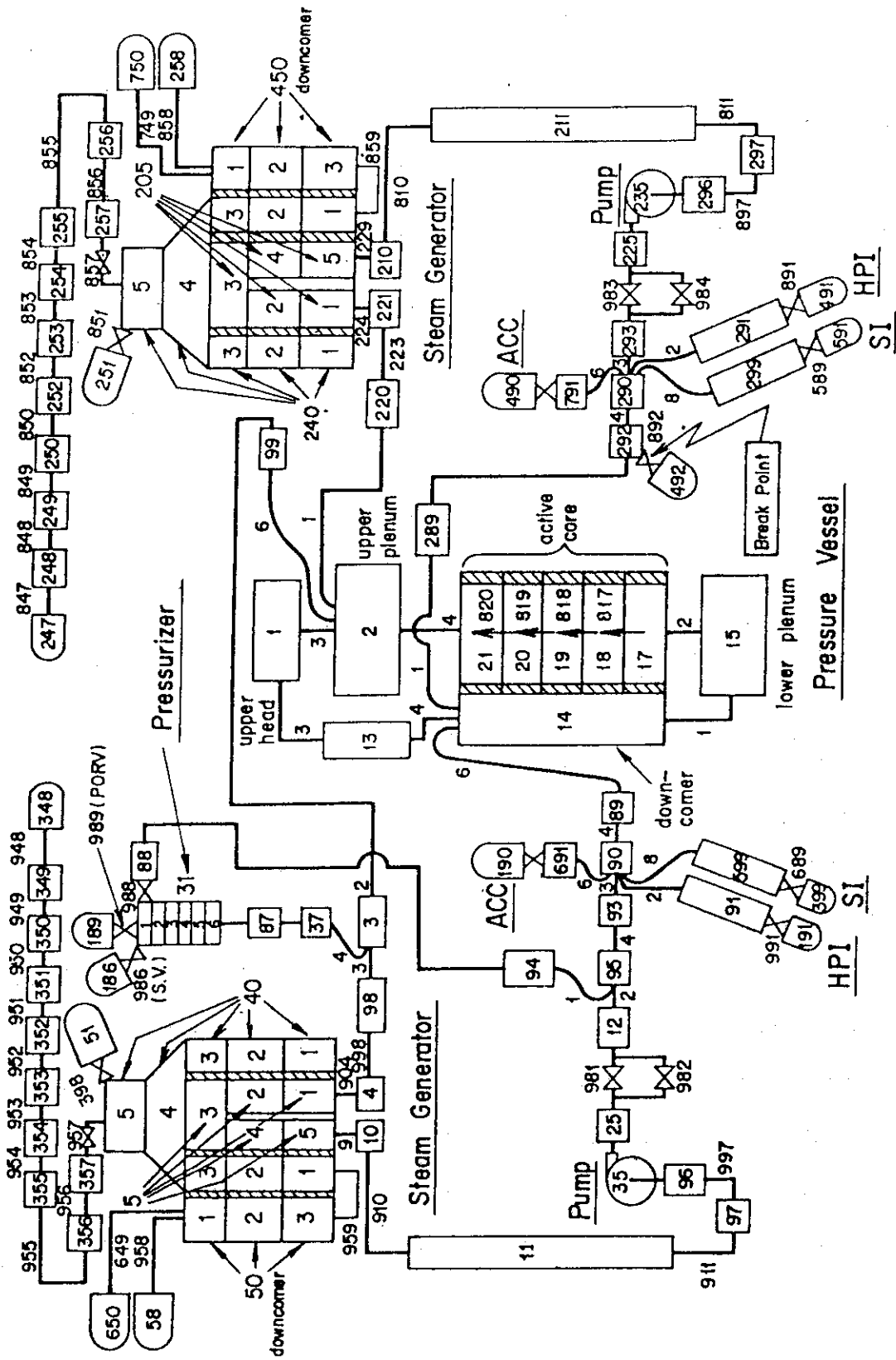


Fig.3.2 Nodalization of LSTF (MOD1 Calculation)

4. ANALYSIS OF CALCULATED RESULTS

This section presents the results of comparing the calculations completed with RELAP5/MOD0 and RELAP5/MOD1, cycle 1. The major new features of RELAP5/MOD1, cycle 1, include: an accumulator model, point kinetics, flow regime maps for horizontal components and annular flow, a generalized control valve, control system, steam separator model and boron concentration model. A noncondensable gas field has been included in the hydrodynamic model and a horizontal stratified flow model has been added to both the hydrodynamic and critical flow models. Significant model improvements include: addition of non-equilibrium effects in the subcooled critical flow model, semi-implicit coupling of the critical flow model, and other code input/output related features. Because the LSTF is a non-nuclear test facility and because it was decided to maintain as much similarity in the input models as possible, of the new models and code improvements listed above only the flow regime map, stratified flow model and critical flow model changes will affect the calculated results. However, the detailed sensitivity study needed to accurately determine the affects of new models, code improvements, and error corrections on the calculated results was beyond the scope of this study and therefore only general conclusions can be drawn from the analysis.

The first section will discuss the comparison of the calculated results for the 10% break and will be followed by the 2.5% break results.

4.1 10% Cold Leg Break Calculations

Table 4.1 lists the time at which significant events in the transient are calculated to occur. This table shows good agreement between the calculations except for the time at which the main steam isolation valve (MSIV) was calculated to close. This occurred at 26.5 s in the MOD0 calculation but at 4.5 s in the MOD1 calculation. Figure 4.1 shows the steam generator in the MOD1 calculation depressurized much more rapidly than in the MOD0 calculation. This was due to a mass flow out the steam generator secondary which was approximately four times the flow calculated by MOD0 (see Fig.4.2).^[a]

The system pressure, because of the many trips which reference it, was an important parameter to compare to determine if there were any significant differences calculated between the two code versions. The system pressures are shown in Figure 4.3. This comparison shows there was little difference

[a] The difference in the mass flows was due to a vapor velocity which was approximately four times higher in the MOD1 calculation when compared to the MOD0 calculation, rather than differences in conditions upstream of the steam generator secondary outlet. Since the same geometry and loss coefficients were used in both calculations and there were no known MOD0/MOD1 differences which would cause this large a difference, the problem was referred to the RELAP5 code development group at the Idaho National Engineering Laboratory (INEL). They said the RELAP5/MOD1, cycle 1, results calculated in this study were correct in that the results were consistent with the RELAP5 input and coding. At this time, however, they were not sure why the MOD0 and MOD1 results were different.^[6] It should also be noted that, at JAERI, both RELAP5/MOD0 and RELAP5/MOD1, cycle 1, are run on a FACOM-200 computer after translating them from the original CDC versions obtained from the INEL. In both cases, sample problems were run with the FACOM computer versions. The results of these sample problems checked out okay when compared to the output from the CDC versions. Therefore, the cause of the difference in the vapor velocity calculated by MOD1 and MOD0 is not known by the authors at this time.

in the calculated pressures although the pressure calculated by MOD1 was a little lower from approximately 8 s to 35 s after rupture. This lower pressure was due to greater energy transfer from the primary to the secondary (see Figure 4.4). The greater energy transfer was a result of the lower secondary pressure in the MOD1 calculation. It could also be due in part to differences in heat transfer models.

The break flow model was improved and new models added to it. The comparison of the break flow calculated by MOD0 and MOD1 is shown in Fig.4.5. This comparison shows that early in the transient the MOD1 calculated break flow was larger than the MOD0 flow and at approximately 22 s the MOD0 flow showed large oscillations which were not calculated by MOD1. In general, in single phase critical flow, the higher the system pressure, the larger the break flow. For these two calculations, however, the reverse situation occurred; the break flow was single-phase (see Figure 4.6) but while the MOD1 system pressure was lower than the MOD0 pressure the MOD1 break flow was larger. Therefore, the differences in the break flow in the first part of the calculation are felt to be the result of break flow modeling differences. In the MOD0 calculation, the break flow was calculated to be unchoked for some time steps after 20 s. This was the cause of the large oscillations in the break flow calculated by MOD0. Unchoking at the break during this time period was unrealistic and improvements to the break flow model in MOD1 resulted in the break flow remaining choked.

A comparison of the MOD0 and MOD1 calculated rod surface temperatures is shown in Figure 4.7. As can be seen from this

figure, both calculations showed the rod surface temperatures followed the saturation temperature until approximately 60 s after rupture. At this time there was a small temperature excursion calculated with MOD0, but none was calculated with MOD1. This difference was due to different hydraulic conditions calculated in the core. This is seen in Figure 4.8 which compares the void fraction in the core for the two calculations. This comparison shows the core volume almost completely voided in the MOD0 calculation, while in the MOD1 calculation the void fraction was not calculated to get above approximately 0.93. It should also be noted that RELAP5 assumes rod dryout to occur for void fractions greater than or equal to 0.96, and that the MOD0 calculation exceeded this criteria while the MOD1 calculation came close (~0.93) but remained below the dryout value. Because of this, different portions of the heat transfer logic were used.

The core inlet flow also showed some differences between the calculations after 35 s (see Figure 4.9). The MOD1 calculation showed a rapid reversal of the flow while the MOD0 calculation also calculated a flow reversal, but it was much more gradual. These flow reversals were due to voiding in the broken loop steam generator downflow which reduced the flow through the broken loop to the break from the pump side. The break conditions however were such that the break flow remained the same. In order to make up for the flow decrease from the pump side of the break, more mass had to come from the vessel. The voiding of the steam generator downflow in the MOD0 calculation was more gradual and therefore the core inlet flow reversal was more

gradual. This difference between the calculations could be due to flow regime map and interfacial drag correlation differences which would affect the calculated slip between the phases in the hot leg and steam generator and therefore the voiding of the steam generator tubes.

Figure 4.10 shows a comparison of the total mass in the primary loop. The data shown in this figure indicates approximately the same amount of mass remained in the system when accumulator injection began (68.5 s in the MOD0 calculation and 85.0 s in the MOD1 calculation). Differences in the system mass reflect the differences in the break flow as calculated by MOD0 and MOD1.

4.2 2.5% Cold Leg Break Calculations

In general the differences in the MOD0 and MOD1 calculated results for a 2.5% break are the same as those already discussed for a 10% break. Therefore only specific differences not seen in the 10% break calculations will be discussed.

Table 4.2 lists the times at which important events in the transient are calculated to occur. This list shows that in addition to the difference in the time for MSIV closure already seen in the 10% break calculations there was a significant difference in the time when accumulator injection began. The difference in the MSIV closure time was for the same reason as in the 10% break calculations - a more rapid depressurization of the steam generator secondary because of a large increase in the calculated steam flow rate (see Figures 4.11 and 4.12).

The difference in the start of accumulator injection was due to a slight change in the calculated depressurization rate in the MOD1 calculation (see Figure 4.13). The comparison in Figure 4.13 shows the system pressures in both calculations had plateaued at a pressure slightly above the accumulator setpoint; however, at 230 s the MOD1 calculation showed the system began to depressurize at a slightly faster rate than the MOD0 calculation. This resulted in accumulator injection beginning at 240 s in the broken loop. The increased depressurization rate calculated by MOD1 was due to condensation in the primary loop and the break flow going two-phase. Figure 4.14 shows a comparison of the vapor mass in the primary loop for the two calculations and the data in this figure indicates the vapor mass in the MOD1 calculation decreased at 230 s. Since the volume upstream of the break did not go two-phase until 239 s (see Figure 4.15), the vapor mass decrease must have been due to condensation in the primary loop. The condensation resulted in a smaller specific volume and, therefore, lowered the system pressure. Once the break flow became two-phase, however, the discharge of a two-phase mixture from the system helped maintain the increased depressurization rate in the MOD1 calculation until the break flow became single-phase again at 248 s.

Other differences in the calculated results in the figures above and in Figures 4.16 to 4.20 are similar to those already discussed for the 10% break calculations and occurred for similar reasons.

Table 4.1 Table of Significant Events (10% Break)

<u>Event</u>	<u>Time (s)</u>	
	<u>MOD 0</u>	<u>MOD 1</u>
Break	0.0	0.0
Scram (PWR)	3.2	2.8
SI Signal	4.0	3.75
LSTF Power Trip	10.3	9.9
SI Begins	21.0	20.8
MSIV Closes	26.5	4.5
Aux FW Begins	32.0	31.8
Accumulator Injection Begins	68.5	85.0

Table 4.2 Table of Significant Events (2.5% Break)

<u>Event</u>	<u>Time (s)</u>	
	<u>MOD 0</u>	<u>MOD 1</u>
Break	0.0	0.0
Scram (PWR)	7.5	6.3
SI Signal	9.4	7.8
LSTF Power Trip	14.6	13.3
MSIV Closes	22.0	5.0
SI Begins	26.4	24.8
Aux FW Begins	37.4	35.8
Accumulator Injection Begins	> 410*	240 (BL) 265 (IL)

* Accumulator injection had not begun when the MOD0 calculation was stopped at 410 s.

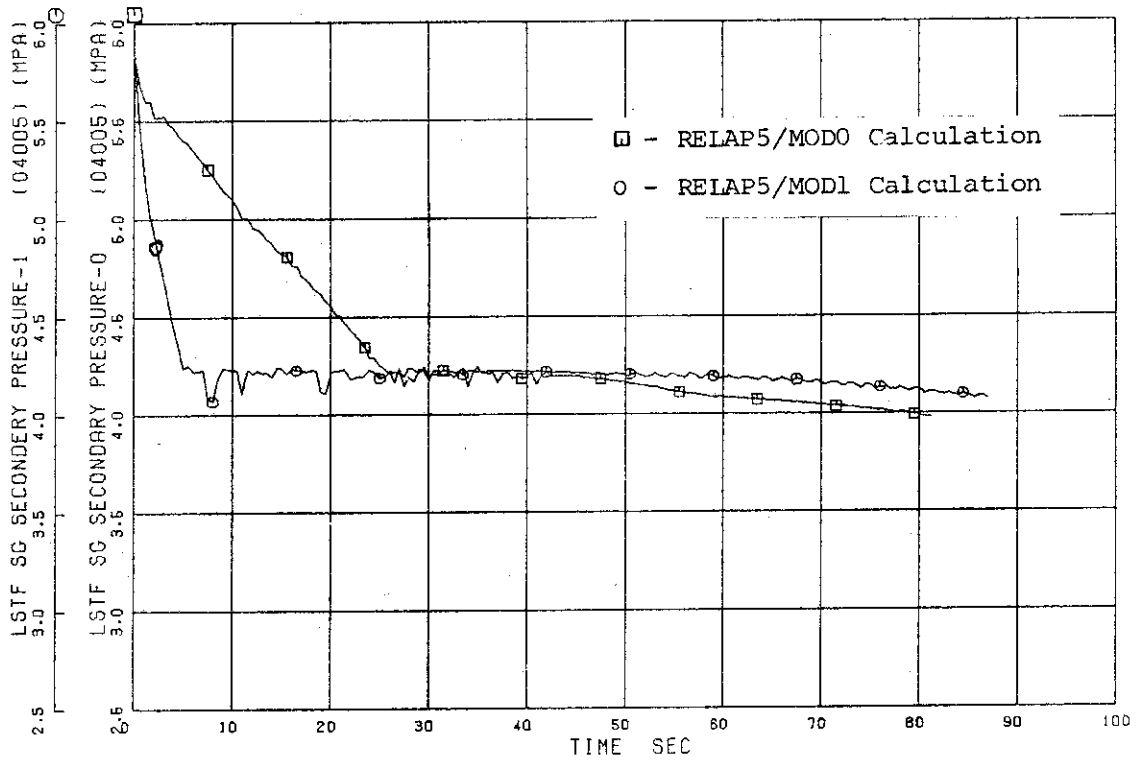


Fig.4.1 Comparison of S.G. Secondary Pressure between MOD0 and MOD1.

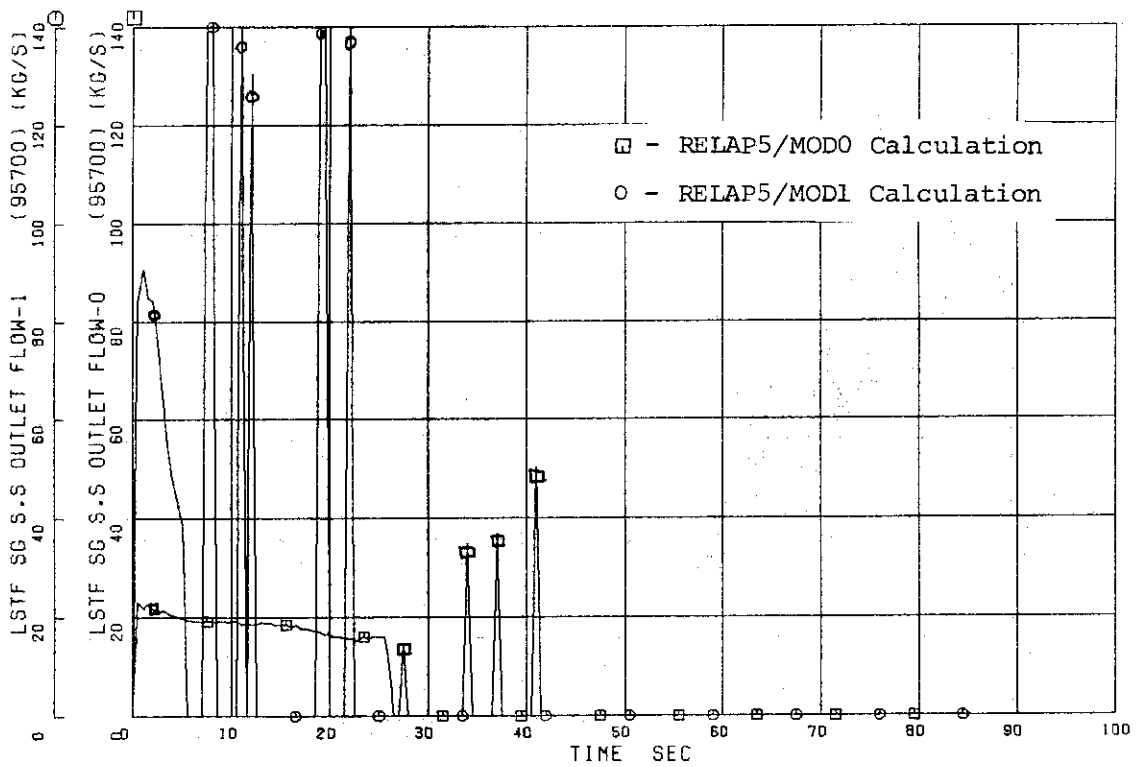


Fig.4.2 Comparison of S.G. Secondary Outlet Flow between MOD0 and MOD1.

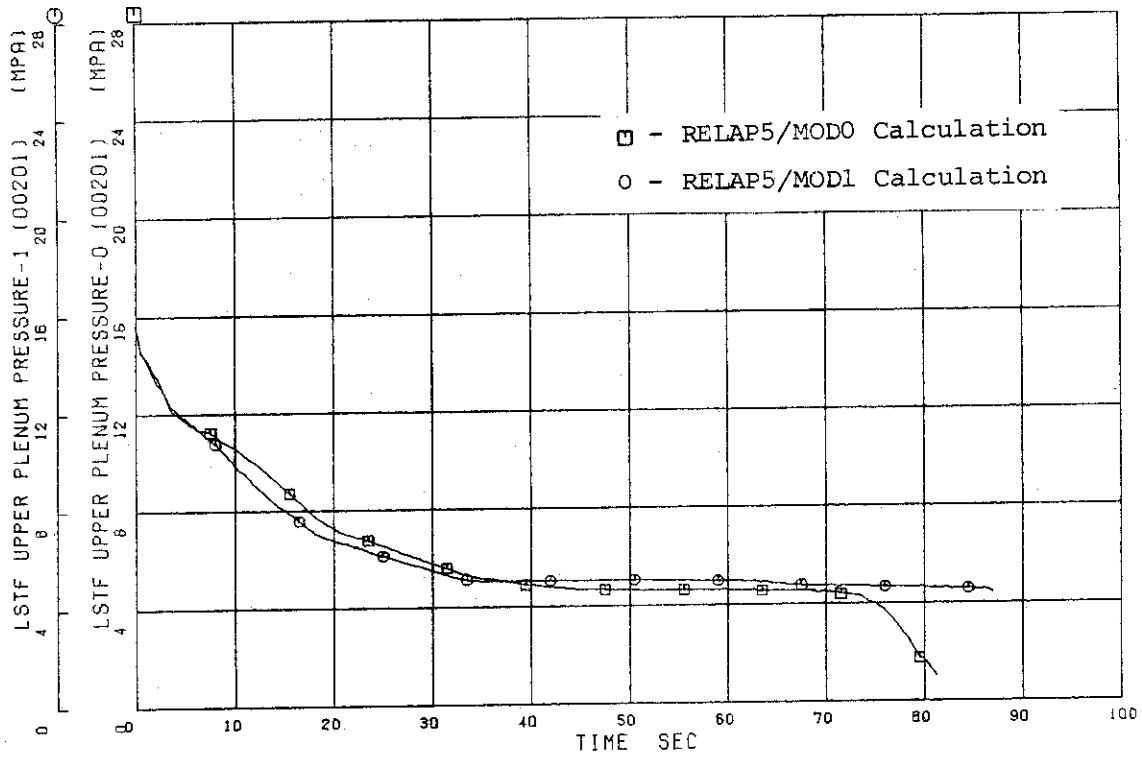


Fig.4.3 Comparison of Upper Plenum Pressure between MOD0 and MOD1.

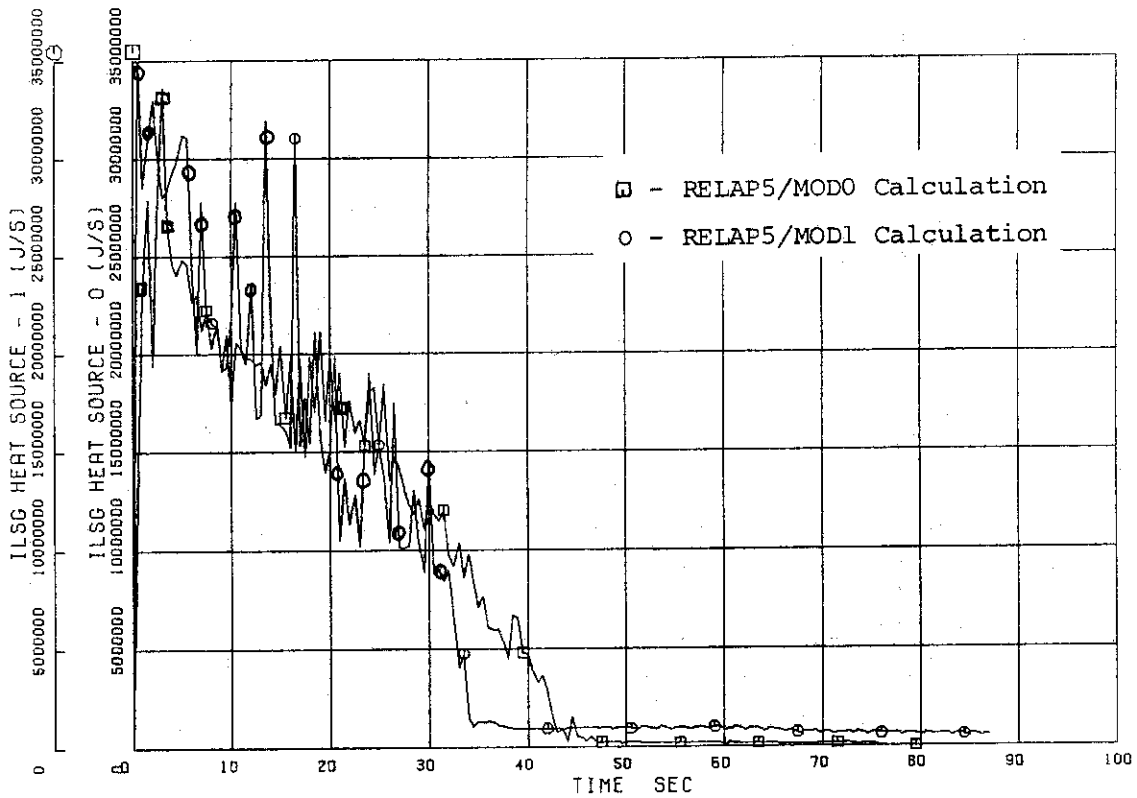


Fig.4.4 Comparison of S.G. Secondary Heat Transfer between MOD0 and MOD1.

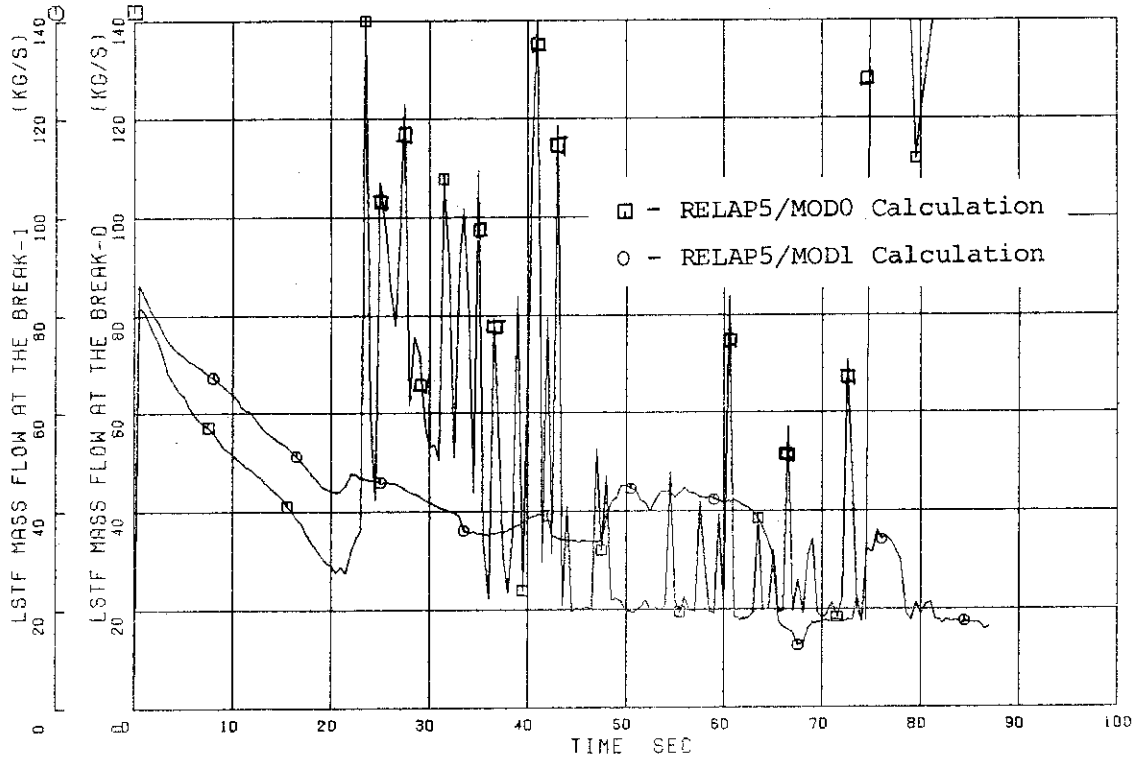


Fig.4.5 Comparison of Break Flow between MOD0 and MOD1.

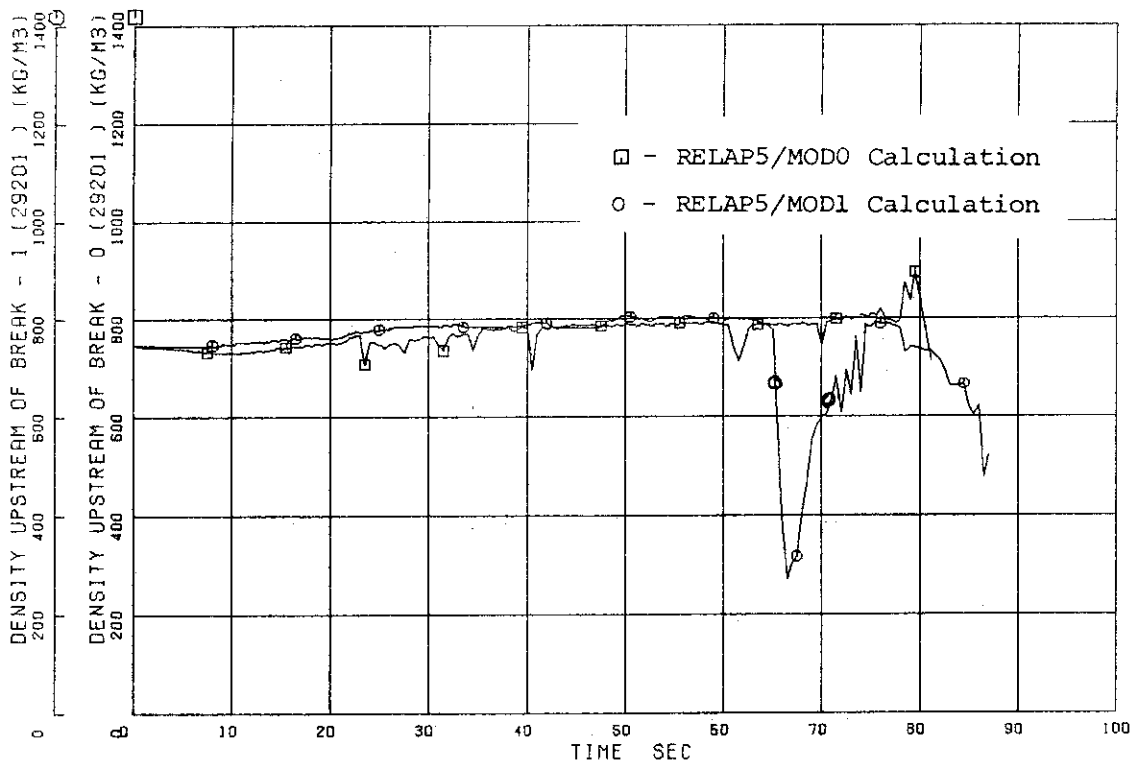


Fig.4.6 Comparison of Density Upstream of the Break between MOD0 and MOD1.

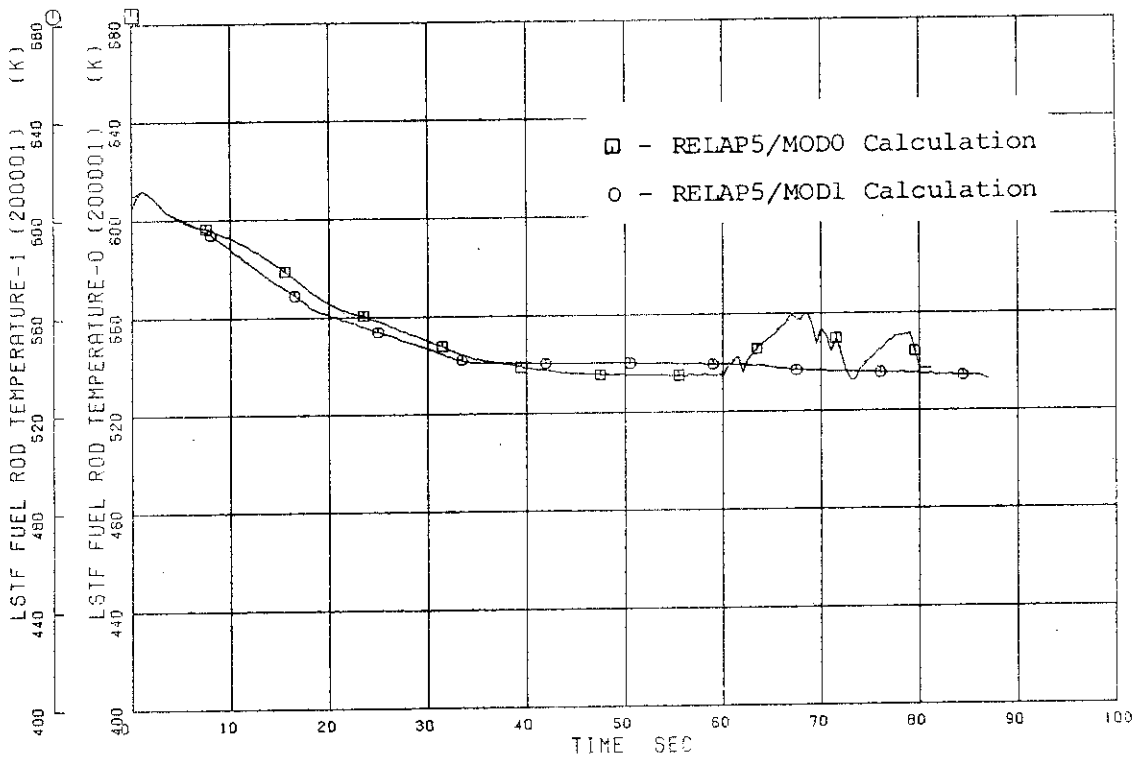


Fig.4.7 Comparison of Rod Surface Temperature between MOD0 and MOD1.

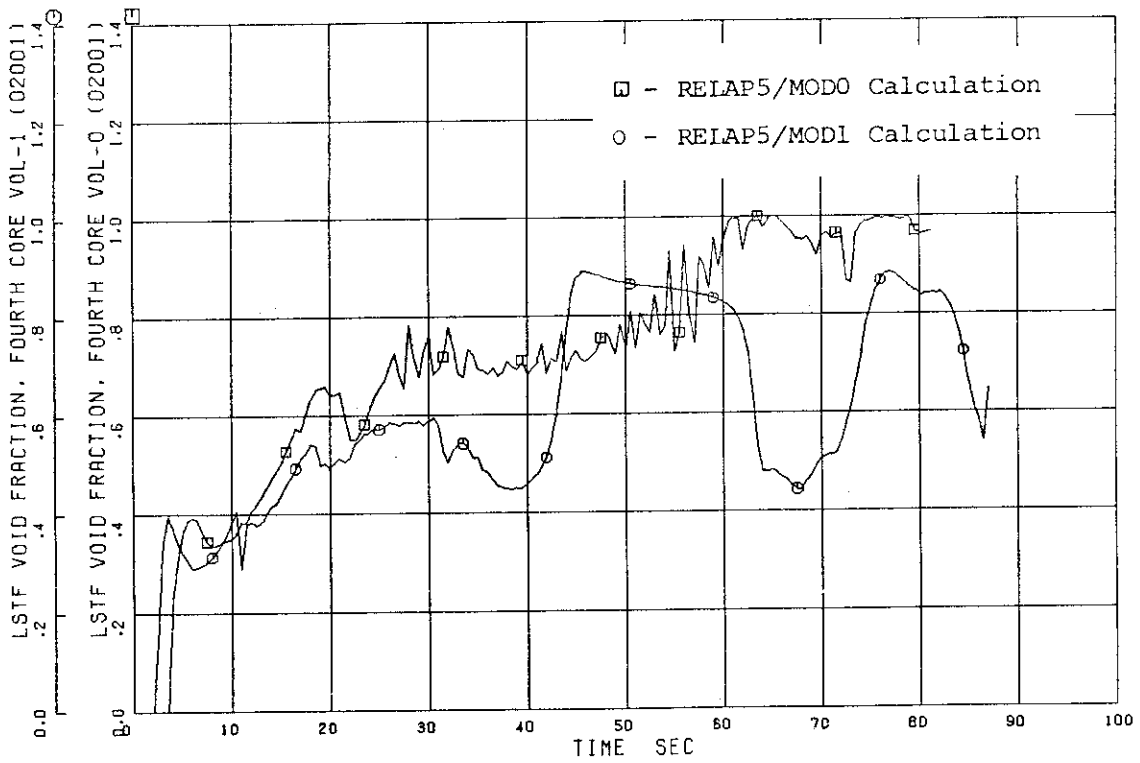


Fig.4.8 Comparison of Void Fraction in the Core between MOD0 and MOD1.

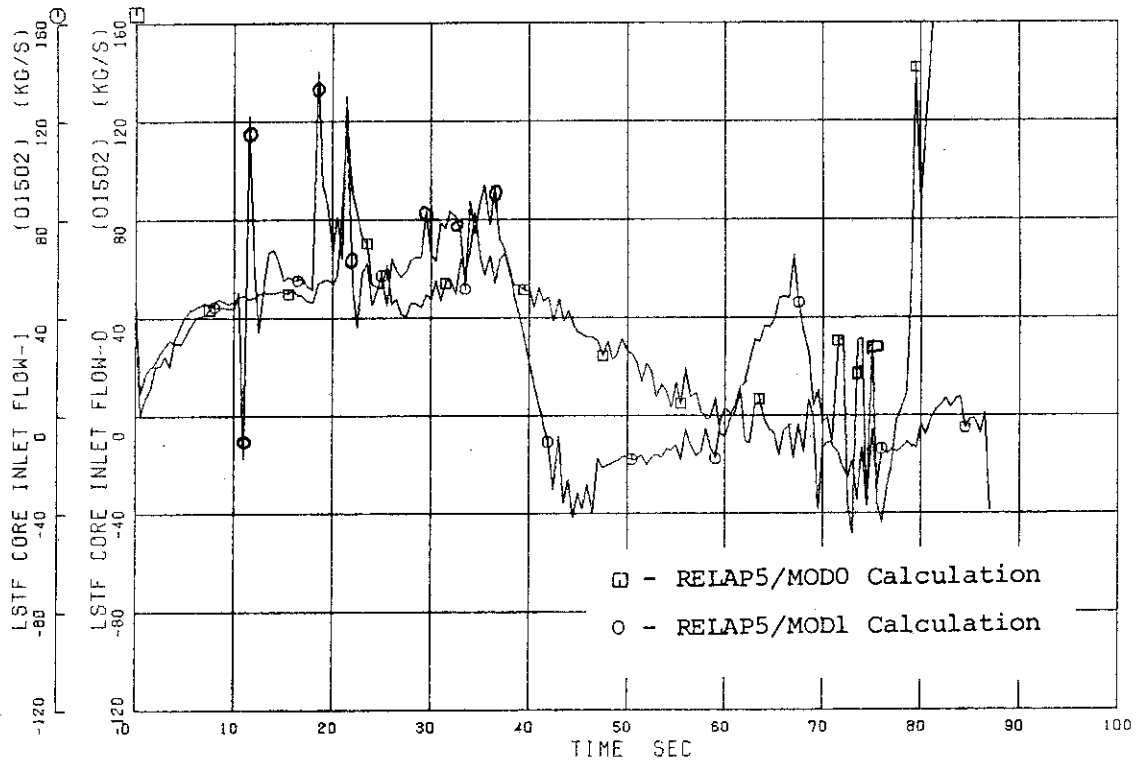


Fig.4.9 Comparison of Core Inlet Flowrate between MOD0 and MOD1.

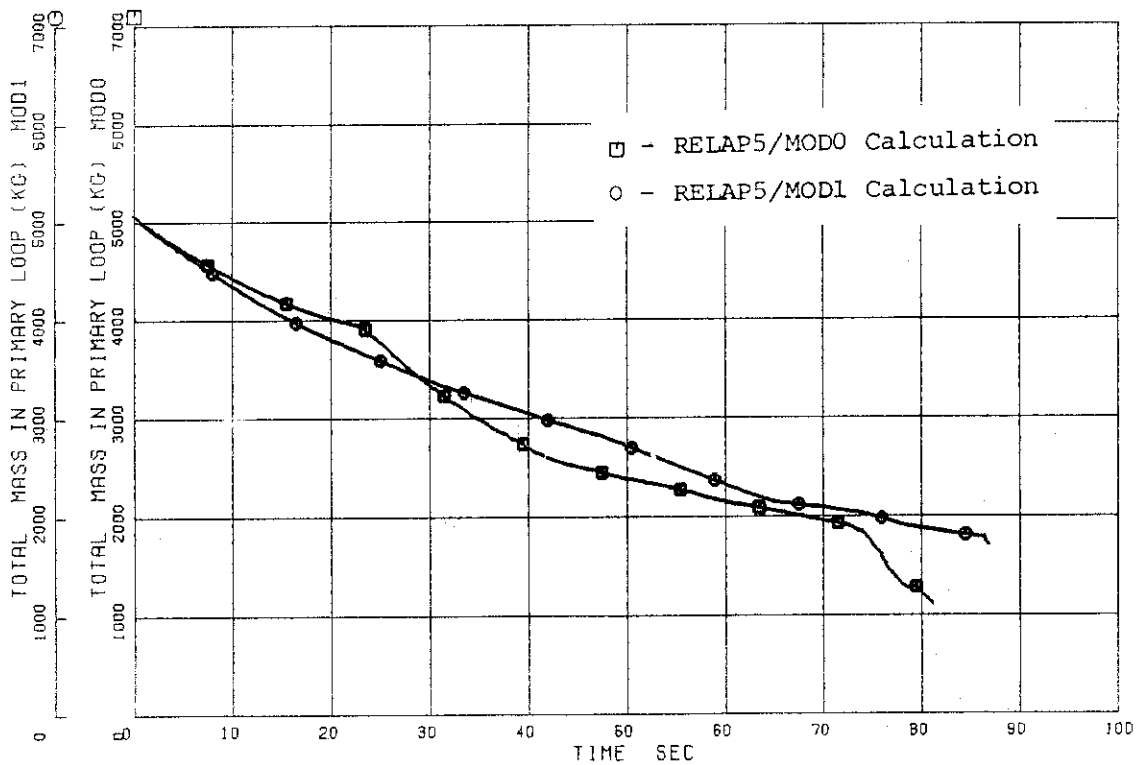


Fig.4.10 Comparison of Total Mass in Primary Loop between MOD0 and MOD1.

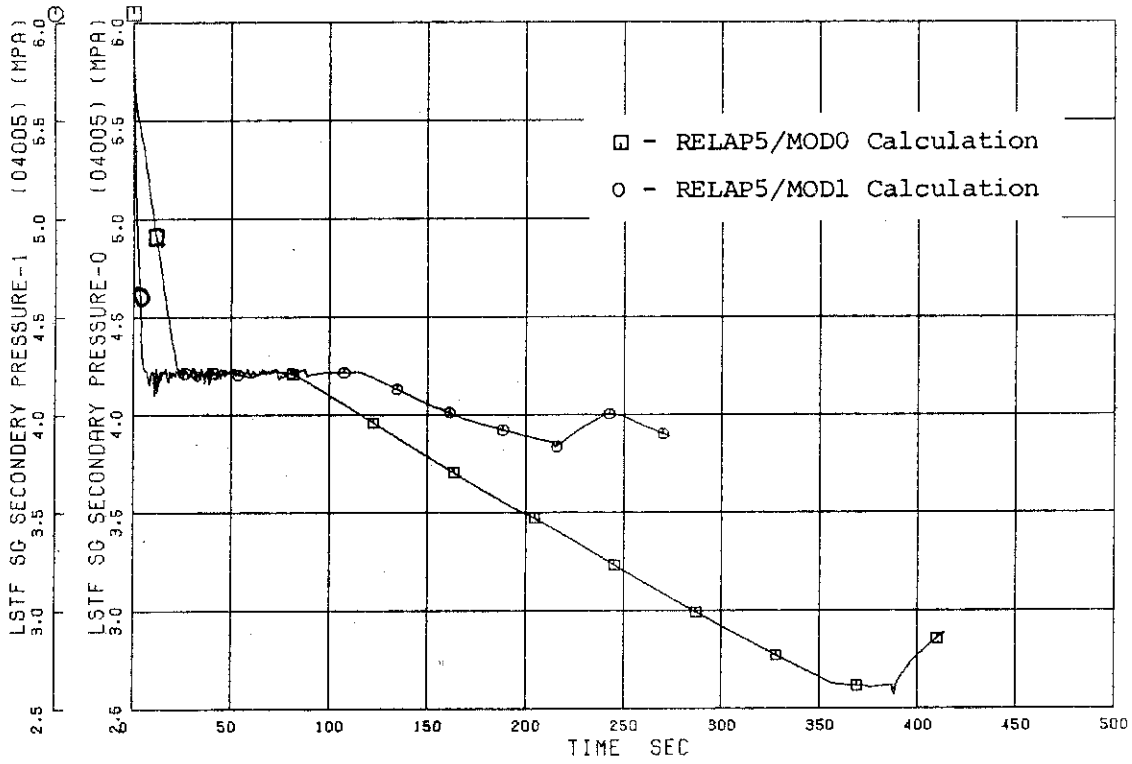


Fig.4.11 Comparison of S.G. Secondary Pressure between MOD0 and MOD1.

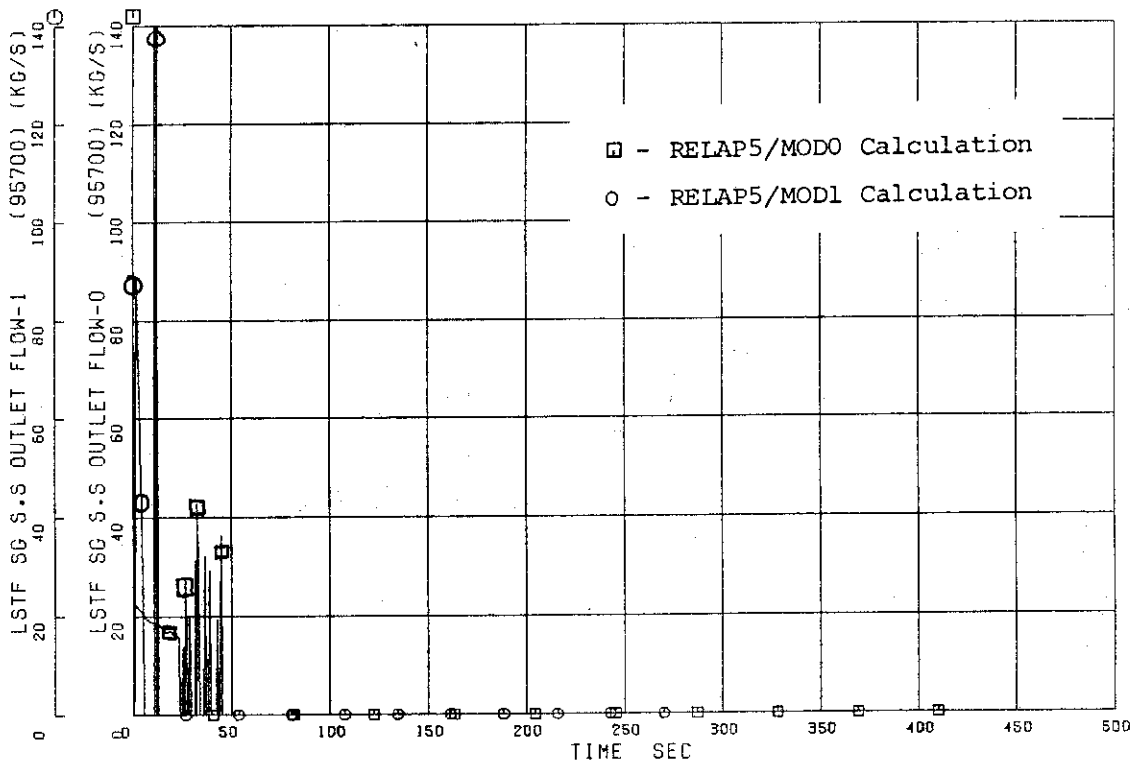


Fig.4.12 Comparison of S.G. Secondary Outlet Flow between MOD0 and MOD1

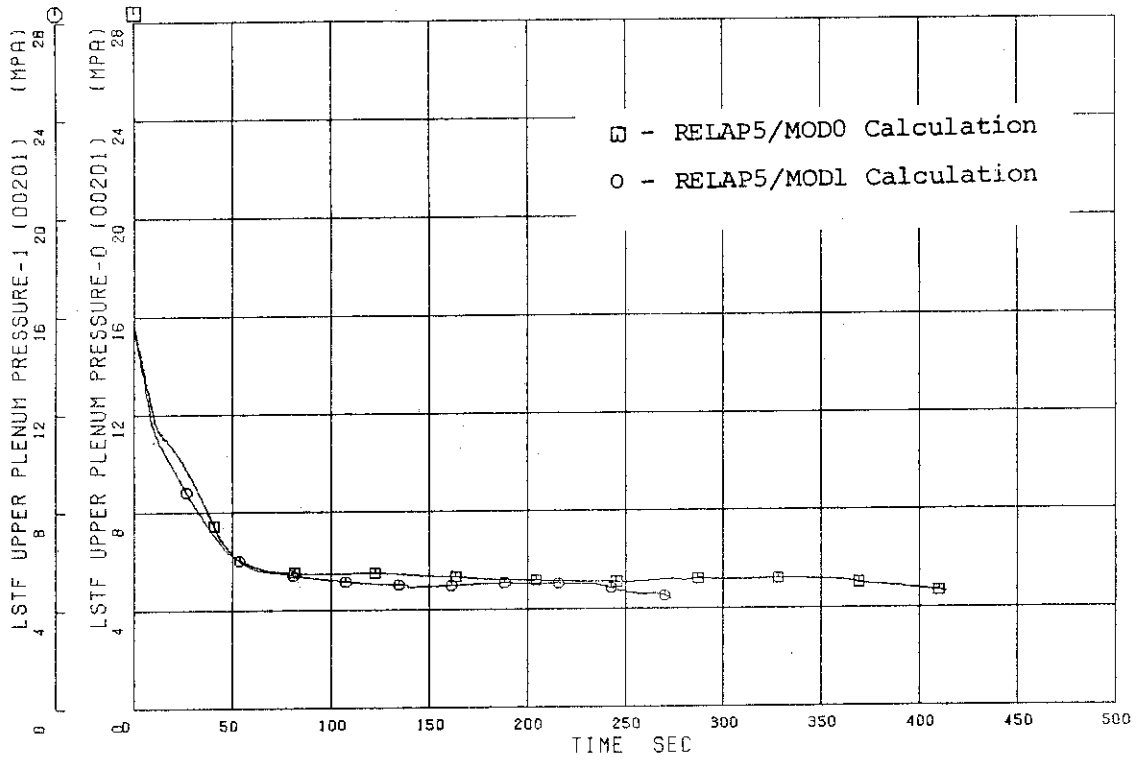


Fig.4.13 Comparison of Upper Plenum Pressure between MOD0 and MOD1.

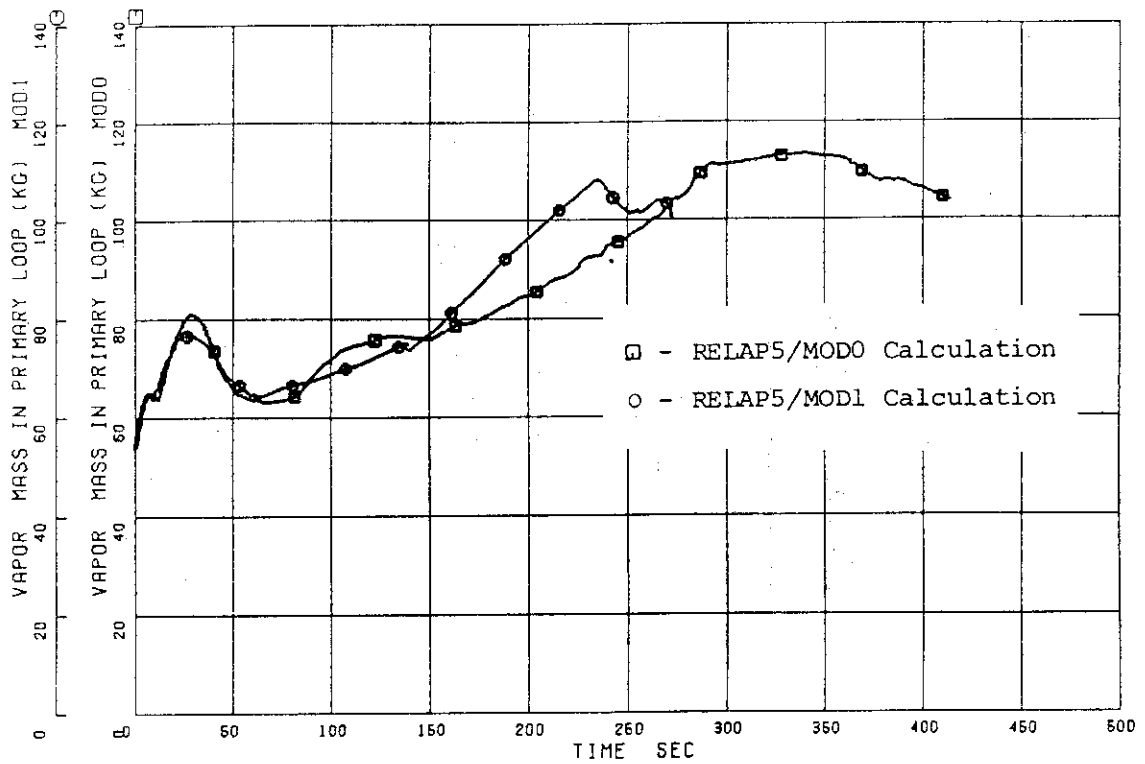


Fig.4.14 Comparison of Vapor Mass in Primary Loop between MOD0 and MOD1.

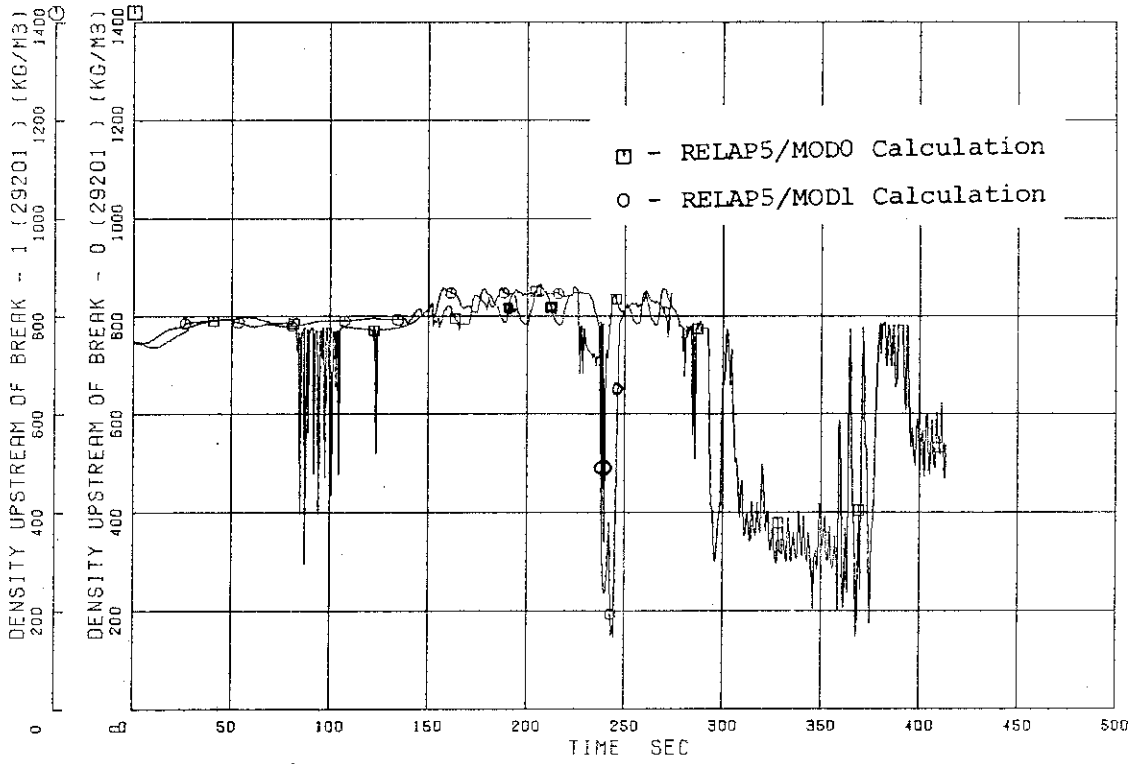


Fig.4.15 Comparison of Density Upstream of the Break between MOD0 and MOD1.

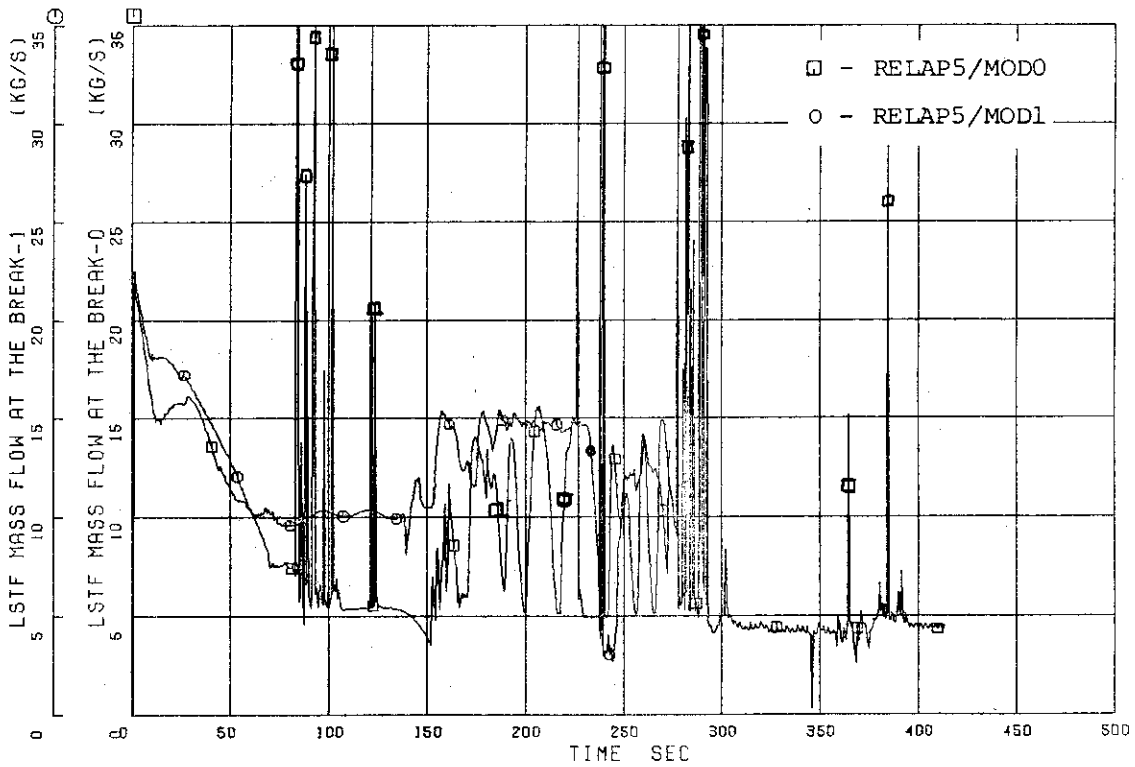


Fig.4.16 Comparison of Break Flowrate between MOD0 and MOD1.

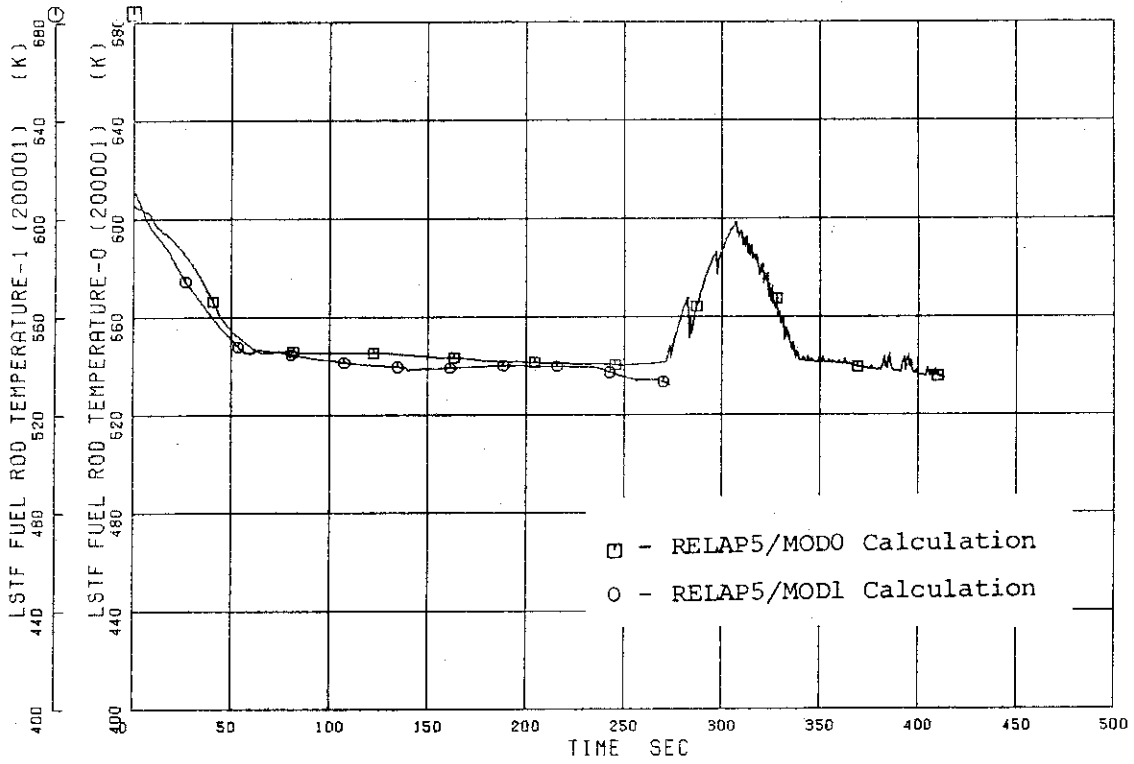


Fig.4.17 Comparison of Rod Surface Temperature between MOD0 and MOD1.

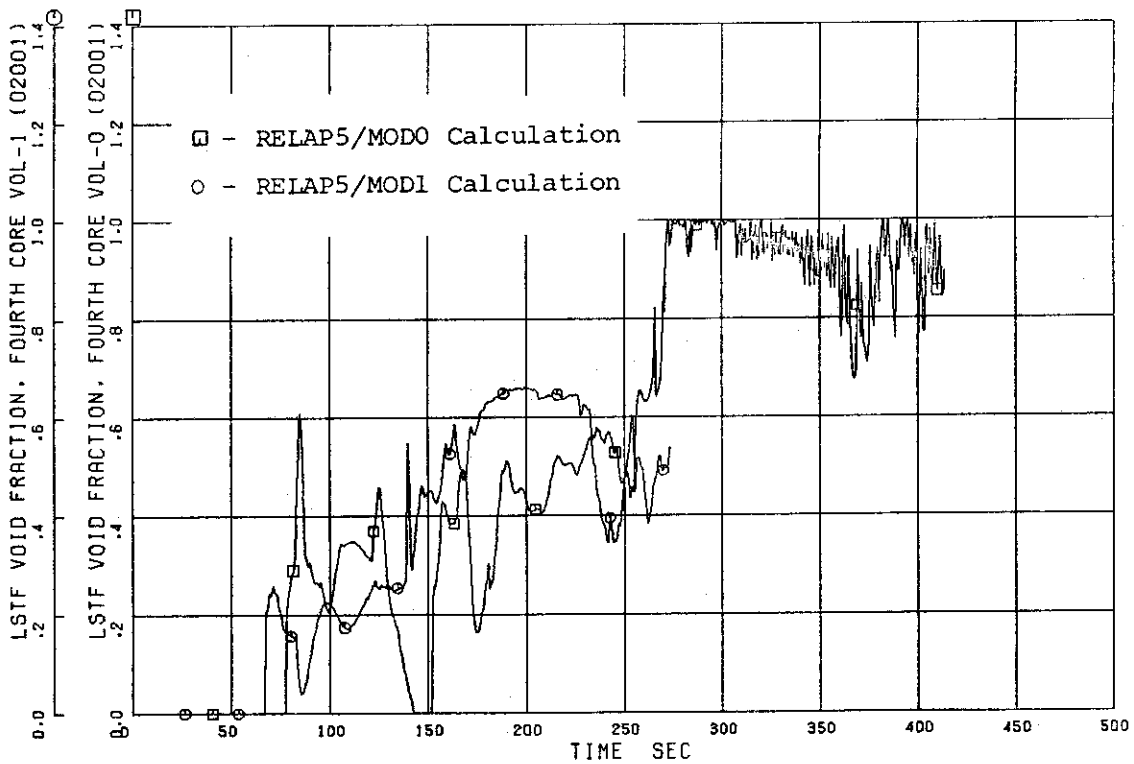


Fig.4.18 Comparison of Void Fraction in the Core between MOD0 and MOD1.

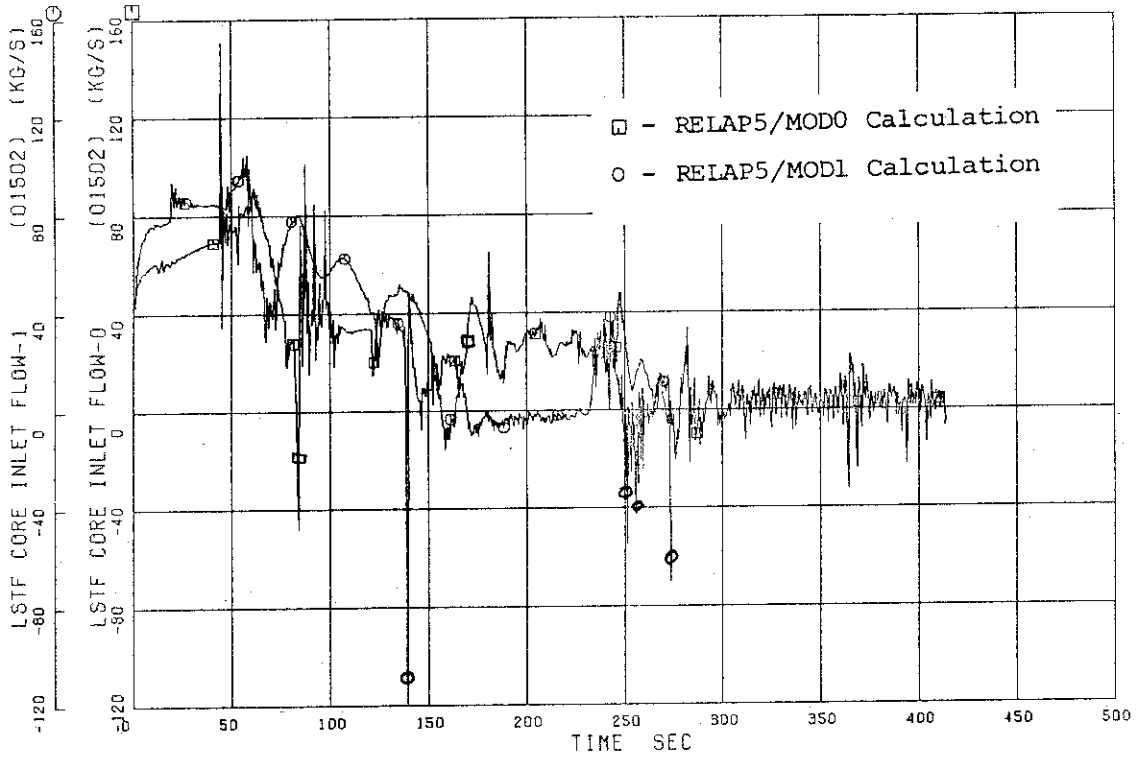


Fig.4.19 Comparison of Core Inlet Flowrate between MOD0 and MOD1.

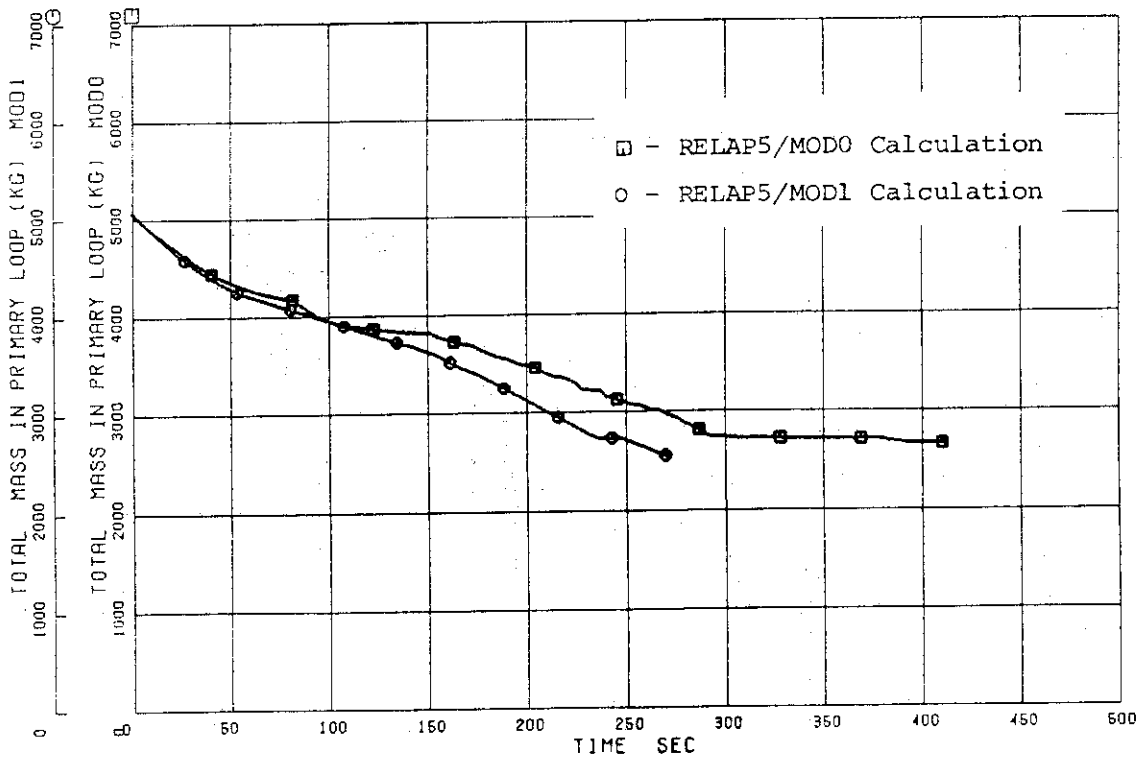


Fig.4.20 Comparison of Total Mass in Primary Loop between MOD0 and MOD1.

5. CONCLUSIONS

Calculations for a 10% and a 2.5% break experiment in the LSTF of the ROSA-IV program have been completed with the RELAP5/MOD0 and RELAP5/MOD1, cycle 1, computer codes. Differences in the two calculations were observed which can be attributed to changes in the flow regime map and critical flow models in the two code versions. In general these differences were not significant. The one exception was the calculation of a transient steam flow from the steam generators which was four times larger in the MOD1 calculation than in the MOD0 calculation even though the same input data was used.

Without experimental data to compare to the calculated results, it is difficult to judge which of the versions of RELAP5 did a better job calculating the response of LSTF. This is especially true since the full range of new models available in RELAP5/MOD1 was not used in order to keep the input models consistent. However, because of the improved physical modeling in RELAP5/MOD1 (for example, a stratified flow model) it is recommended that RELAP5/MOD1, cycle 1, and later versions of RELAP5/MOD1 as they become available, be used in the analysis of LSTF experiments.

ACKNOWLEDGEMENTS

The authors would like to thank Mr. K. Yamano for his valuable assistance in completing the RELAP5 calculations and in preparing the figures for this report.

5. CONCLUSIONS

Calculations for a 10% and a 2.5% break experiment in the LSTF of the ROSA-IV program have been completed with the RELAP5/MOD0 and RELAP5/MOD1, cycle 1, computer codes. Differences in the two calculations were observed which can be attributed to changes in the flow regime map and critical flow models in the two code versions. In general these differences were not significant. The one exception was the calculation of a transient steam flow from the steam generators which was four times larger in the MOD1 calculation than in the MOD0 calculation even though the same input data was used.

Without experimental data to compare to the calculated results, it is difficult to judge which of the versions of RELAP5 did a better job calculating the response of LSTF. This is especially true since the full range of new models available in RELAP5/MOD1 was not used in order to keep the input models consistent. However, because of the improved physical modeling in RELAP5/MOD1 (for example, a stratified flow model) it is recommended that RELAP5/MOD1, cycle 1, and later versions of RELAP5/MOD1 as they become available, be used in the analysis of LSTF experiments.

ACKNOWLEDGEMENTS

The authors would like to thank Mr. K. Yamano for his valuable assistance in completing the RELAP5 calculations and in preparing the figures for this report.

REFERENCES

- 1) Tasaka, K. et al.: "Conceptual Design of Large Scale Test Facility (LSTF) of ROSA-IV Program for PWR Small Break LOCA Integral Experiment," JAERI-M 9849 (1981).
- 2) Ransom, V.H., et al.: "RELAP5/MOD0 Code Description, Volume 1, 2, 3," CD-TR-057, (1979).
- 3) Tanaka, M., Katada, K., and Tasaka, K.: "Preanalysis of ROSA-IV LSTF for PWR Small-Break LOCA Test with RELAP5/MOD0-10% Cold Leg Break with HPI Failure," JAERI-M 9356 (1981).
- 4) Tanaka, M., Katada, K., and Tasaka, K.: "Preanalysis of ROSA-IV LSTF for PWR Small-Break LOCA Test with RELAP5/MOD0-2.5% Cold Leg Break with HPI Failure," JAERI-M 9676 (1981).
- 5) Ransom, V.H., et al.: "RELAP5/MOD1 Code Manual, Volume 1, 2, 3 (Draft)," EGG-2070 (1980).
- 6) Private Communication with the RELAP5 Code Development Group.